Resonantly induced transparency for metals with low angular dependence

Miguel Camacho, Alastair P. Hibbins, and J. Roy Sambles

Citation: Appl. Phys. Lett. **109**, 241601 (2016); doi: 10.1063/1.4971983
View online: http://dx.doi.org/10.1063/1.4971983
View Table of Contents: http://aip.scitation.org/toc/apl/109/24
Published by the American Institute of Physics

Resonantly induced transparency for metals with low angular dependence

Miguel Camacho,[a] Alastair P. Hibbins, and J. Roy Sambles
Electromagnetic and Acoustic Materials Group, Department of Physics and Astronomy, University of Exeter, Stocker Road, Exeter EX4 4QL, United Kingdom

(Received 13 September 2016; accepted 28 November 2016; published online 15 December 2016)

Thin (sub skin-depth) metal layers are known to almost completely reflect radiation at microwave frequencies. It has previously been shown that this can be overcome at resonance via the addition of closely spaced periodic structures on either side of the film. In this work, we have extended the original one-dimensional impedance mechanism to the use of two-dimensional periodic structures both experimentally and analytically using an equivalent circuit approach. The resulting device shows experimentally a low (<5% relative frequency shift) dependence in both angle of incidence and polarisation. We also show that the same principle can be used to transmit through a thicker ($\sim\mu$m) perfectly conducting film perforated with a non-diffracting (short pitch) array of subwavelength holes with the cut-off frequency above 900 GHz showing resonant transmissivities in the 20–30 GHz range above 40%. [http://dx.doi.org/10.1063/1.4971983]

At microwave frequencies, in contrast to the plasma-like behaviour of metals at visible frequencies, metals behave as near perfect electric conductors (PECs). They efficiently screen the electric field, resulting in a skin depth of $\sim 1\ \mu$m. For metals with thickness greater than this, the limited penetration of the electric fields results in a zero transmittance while, for thicknesses below the skin depth, the impedance mismatch with respect to free space limits the transmittance to negligible values (this opacity of metals is not only limited to the microwave range, and transmission through such layers can be treated as a tunneling problem at visible frequencies due to the high and negative value of the real part of their permittivity.)[1]

However, it has been shown that for thicknesses below the skin depth this impedance mismatch can be overcome for a specific linear polarisation by surrounding the metal film by one-dimensional arrays of metal strips and hence creating resonant cavities between the surfaces that provide an impedance matching mechanism.[2] In this, the thin metal layer behaves much as a very lossy thin film inside a cavity, in which modes are excited by the diffracted fields on the edges of the metal strips.[3] However, this concept has only been exploited for one dimensional periodic structures, which are strongly polarisation dependent. It can be easily extended to two-dimensional arrays of patches. Due to the resonant nature of the transmission mechanism, impedance matching can only be achieved for a discrete set of frequencies given by the modes of the cavities, resulting in a structure that works as a spatial microwave filter. These types of structures are frequency selective surfaces (FSS)[4] that have been of much interest to the microwave community given their huge number of applications.

Analytical methods have been developed to efficiently predict the behaviour of FSSs. Included in these are method of moments[5] and mode-matching.[6] However, the complexity of the previously cited methods makes them suitable only for modelling electrically big structures. In contrast, analytical equivalent circuits provide us with a very versatile and powerful method that also keeps the simplicity of the analysis of electric circuits including cascaded transmission lines and lumped elements. This method has been recently used by Molero *et al.*[7] to compute the transmission through the one dimensional system, in which they took into account the interaction of the evanescent modes (all of them below cut-off at the frequency range studied) excited by the strip array with the thin metal layer. To compute these interactions, they introduced the slab of thin metal layer contained in the unit cell into the model as a resistor given by $R = 1/(\sigma m_t)$, where σ represents the conductivity of the layer and m_t its thickness. In their original study, Edmunds *et al.*[2] used finite element method (FEM) modelling to predict the response of the structure. Due to the huge number of tetrahedra needed to solve the fields inside the thin metal film (aspect ratio greater than 6×10^4 if the resonance is within the tens of GHz range), an extensive study of the transmissivity for different metal thicknesses is prohibitively computationally expensive using the FEM method; therefore, the efficient analytical technique of circuit equivalence is highly beneficial.

In this study, we extend the work of Edmunds *et al.*[2] into the use of two-dimensional arrays, using the square arrays of patches surrounding the metal film. Given the low angle of incidence dependence of the behaviour of the patch arrays due to the narrow gaps between them and the connectivity of the metal film, our device allows resonant transmission of microwave radiation into a thermally and optically isolated region that may find useful applications in various communication and defence industries as a very thin (smaller than $\lambda_0/100$ at the transmission peak) lightweight, opaque and conductive radome.

Let us start by considering the cavity enhanced transmission through a homogeneous thin metal layer. We have

[a]Electronic mail: mc586@exeter.ac.uk

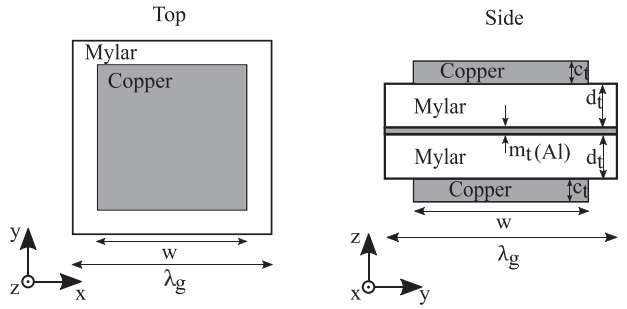

FIG. 1. Top and side views of the unit cell of the system comprising a homogeneous thin metal layer of thickness m_t. The values of the parameters for the experiment are $\lambda_g = 3.8$ mm, $w = 3.6$ mm, $d_t = 75\ \mu$m, $m_t = 60$ nm and $c_t = 17\ \mu$m.

made use of the structure represented in Fig. 1, in which a 60 nm aluminised plastic layer is symmetrically sandwiched between two periodic square arrays of metal patches. For the sake of simplicity, this figure does not show the two perspex layers placed on either side of the structure, required to hold these layers together. The physical phenomenon behind the impedance matching mechanism is the spatial separation of the maximum B and E fields in the cavity created between the top and bottom patches. This way, maximum B field is found under the centre of the patches and the maximum E field is located in the vicinity of the edges of the patches. This electromagnetic field decomposition allows us to excite waveguide modes with a range of wave impedances, allowing transmission through a very good conductive layer, which has negligible impedance. The field distribution is represented in Fig. 2.

To quantitatively determine the frequency dependent transmission through this multi-layered system, we have made use of both equivalent circuit and FEM modelling as a validation technique. For the former, we used the equivalent circuit model presented by Molero *et al.*[7] to calculate the admittance of the slits per unit length as an infinite series of the admittances seen either side of them by all the modes excited by the scattering of the impinging plane wave. Given the fact that the two resonant patch arrays are placed symmetrically with respect to the center of the system, the even-odd excitation decomposition can be applied, resulting in the equivalent circuits shown in Fig. 3. In this, the wave arriving from only one side of the system ($z \to +\infty$ or $z \to -\infty$) is decomposed into the sum of two excitations impinging from both terminals, for which the plane $z = 0$ behaves as an electric wall (for odd excitation) or as a magnetic wall (for even excitation). These walls correspond to a short circuit or open circuit termination, respectively, allowing us to obtain the total transmission coefficient (in amplitude) from the sum of the reflection coefficients of the circuits shown in Fig. 3. Each of these solutions can be computed analytically to a high degree of accuracy following the work of Rodríguez-Berral *et al.*[8] using a single basis function for the electric field between the edges of the patches when including the right behaviour near the edges. To account for the shorter length of the side of the patches compared to the side of the unit cell, we have multiplied the obtained admittance (and therefore the corresponding capacitance of the patches) by a factor of $\frac{w}{\lambda_g}$. Given that the slits are very narrow, this factor is close to 1 but important for obtaining the right resonance frequency (if this factor is made equal to 1, the behaviour of the 1D system is recovered). For the same reason, we are able to neglect the admittance associated with the slits parallel to the impinging electric field given that the electric field must be zero near the edge of the patch and hence the modes excited by the scattering of the wave by those slits have a negligible amplitude.[8] This same model can also be used to study oblique incidence by introducing an extra in-plane momentum component in the infinite series involved in the calculation of the admittance of the slits for both transverse electric (TE) and magnetic (TM) components of the incident wave, for each of which the corresponding angle dependent impedance has to be calculated for the media surrounding the slits. In Fig. 4, we show the high degree of agreement between the analytical circuit model and the FEM modelling. This purely analytical equivalent circuit model does not

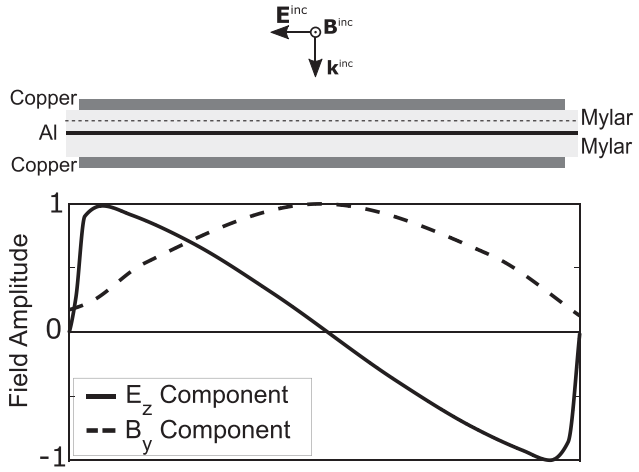

FIG. 2. Predicted normalized field distribution in the cavity formed in the middle plane between the patch and the thin metal layer (dashed line on the top art) at the resonant frequency obtained from FEM simulation. The electric and magnetic field maxima appear at different positions, hence allowing the impedance matching between free space and the highly conductive layer.

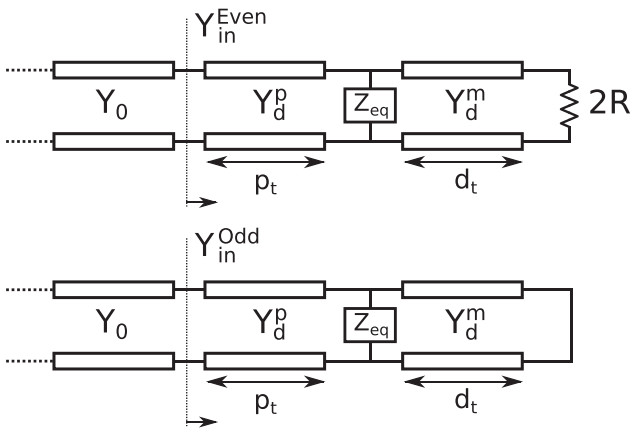

FIG. 3. Equivalent circuits computed for the even-odd excitation decomposition of the system shown in Fig. 1. Transmission line sections represent the dielectric slabs within the system (Y_d^p and Y_d^m being the impedance of the perspex and the copper coated plastic layers, respectively) and Z_{eq} and R represent the equivalent lumped element representing the patch array and the thin metal layer, respectively.

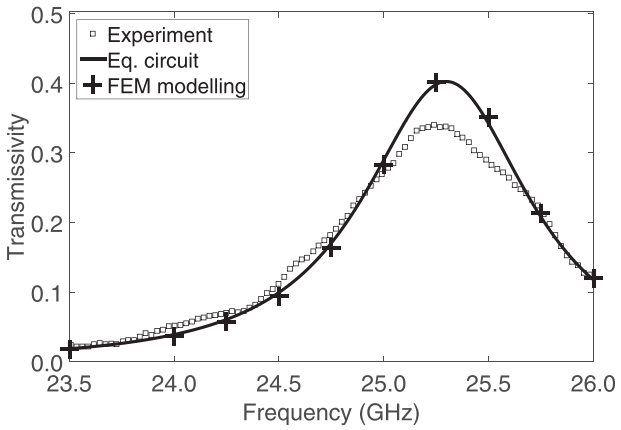

FIG. 4. Experimental transmissivity for normal incidence with the FEM modelling and circuit model predictions for the homogeneous thin metal film and sample parameters, as specified in the caption of Fig. 1.

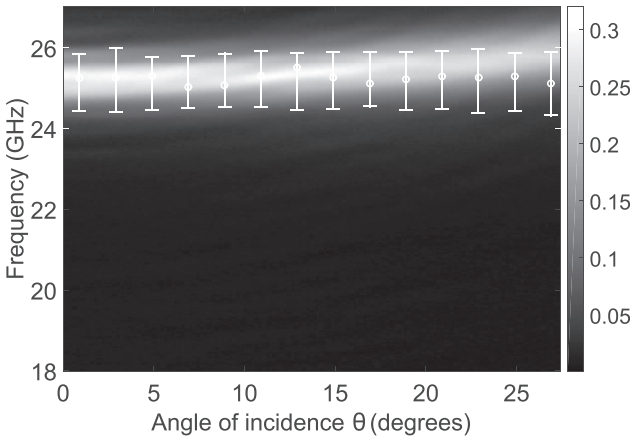

FIG. 5. Experimental transmissivity for TM (background gray scale) and TE (superimposed circles with error bars representing the frequency interval over which the transmissivity is at least half of that of the maximum at that angle) polarisations for angles θ between 0° and 27°.

require any fitting parameter and therefore does not rely on any full wave analysis of the structure.

To test the validity of the results obtained from our equivalent circuit model and also from the FEM model,[9] we have undertaken an experiment for $m_t = 60$ nm. For the fabrication of the arrays of patches, we used a print and etch technique, which consists of printing the desired pattern using ferric-chloride-resistant ink and etching the not-printed part of the surface, applied to flexible 75 μm thick plastic layers coated with a 17 μm thick copper layer. The value of the dielectric constant for the plastic layers used was 2.6 with a negligible imaginary part. The size of the sample was $25 \times 16\,\text{cm}^2$. To minimize thin gaps of air between the layers comprising the sample, two 7.44 mm thick perspex layers were added on either side to compress the structure. The dielectric constant for these layers is $2.6 + 0.015i$. The values for thicknesses and dielectric constants are consistent with the previous work done using the same materials.[2] These complex dielectric constants are taken into account in the equivalent circuit model when calculating the impedance and propagation constant associated with the transmission line sections in Fig. 3. We have obtained experimentally a well defined transmissivity peak with a relative bandwidth of 4%. The results show the best agreement with both FEM and circuit modelling predictions when a 10 ± 2 μm air layer is included between the homogeneous layer and the dielectric spacer to take into account the residual small air gaps between the polymer layers. These air gaps are responsible for a shift of the resonant frequency towards higher frequencies of less than 4%. We find that to obtain the experimental transmissivity maximum for a 60 nm thick aluminium layer, a conductivity of $\sigma = 1.65 \times 10^7$ S/m has to be introduced, this being nearly half of the conductivity for bulk aluminium. This is in agreement with what is expected[10] due to the surface scattering of the electrons.

We have also studied the angle (θ) dependence of the transmission peak for both transverse electric (TE) and magnetic (TM) polarisations for $0° < \theta < 27°$ (Fig. 5), the angle range being limited by the small size of the sample. For TM polarisation, the transmission maximum is shifted up in frequency by less than 5% at 27° with respect to normal incidence, which is of the order of the relative bandwidth of the transmission peak. However, for TE polarisation, the frequency of the resonance is much less dependent on the angle of incidence, presenting a shift smaller than 1% within the angle interval studied. This is due to the fact that the modes are excited by electric fields perpendicular to the slits, which means that for TE polarisation they are excited in phase for any angle of incidence. However, for TM polarisation, a phase difference is imposed between the slits at either side of a patch increasing the resonant frequency. In addition, the symmetry between $\hat{\mathbf{x}}$ and $\hat{\mathbf{y}}$ directions along the patch array makes the response of the system independent of azimuthal rotations, which in addition to the low dependence on the polarisation shown before makes this device suitable for microwave filtering.

Having studied the resonant transmission through a 60 nm thin continuous metal layers, we have also studied the effect of increasing the metal thickness. In the equivalent circuit, for thicknesses below the skin depth, we represent the thin metal layer as a lumped resistor, whose value R is given by $R = 1/(\sigma m_t)$. The evolution of the modelled transmissivity with R is presented in Fig. 6. It shows that transmissivity

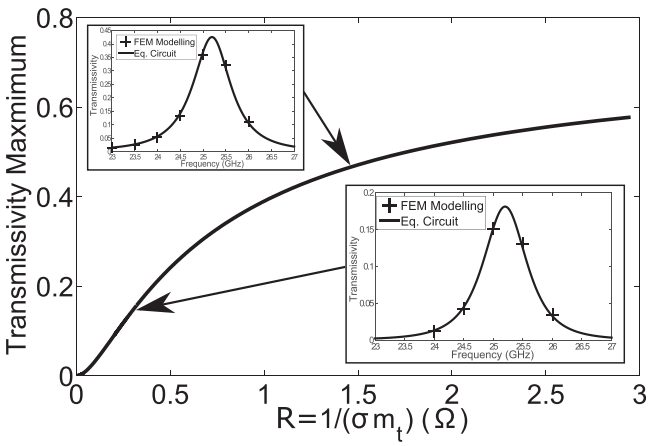

FIG. 6. Predicted dependence of the transmissivity maximum for a continuous thin metal layer of conductivity σ and thickness m_t using the circuit model. Inset: Validation of the results obtained from the circuit model by comparison to FEM modelling for $m_t = 50$ nm (top left) and $m_t = 150$ nm (bottom right) for a conductivity of 1.65×10^7 S/m.

peaks above twenty percent can only be achieved when the equivalent resistor associated with the metal slab in the unit cell is above 0.5 Ω, which means that for aluminium, the thickness needs to be under 300 nm for the conductivity, previously used, of 1.65×10^7 S/m. The fall of the transmission maximum with $1/(\sigma m_t)$ is consistent with the nearly PEC behaviour of metal layers for thicknesses similar to the skin depth. The two insets of Fig. 6 confirm the validity of the model for $m_t = 50$ nm and $m_t = 150$ nm (for a conductivity of 1.65×10^7 S/m) by comparison with the FEM predictions. Although the lumped element approximation explains the fall in the transmission for layers thicknesses similar to the skin depth, it has been found that the behaviour of the conductive layer can no longer be described as a lumped resistor (that assumes a homogeneous current density inside the layer) when the thickness exceeds half of the value of the skin depth, being necessary to take into account the propagation of the fields through the metal.

To illustrate that the two-dimensional resonant impedance matching device presented in this paper is not only limited to highly conductive layers but can be also applied to other impedance mismatch problems, we have replaced the continuous film with a 17 μm one perforated with a 9×9 array of holes per unit cell of the patch array (Fig. 7).

Following the experimental discovery of extraordinary optical transmission,[11] it has been established that microwave transmission is allowed through the arrays of very subwavelength holes due to the reactive behaviour of the surface just below the hole cut-off that allows the impedance of the array to match that of free space.[12] In addition to this, other mechanisms to enhance the transmission have been studied, like cavity resonances in thick (of the order of the wavelength) screens and groove reemission for structured metals.[13] However, for wavelengths, much above the periodicity of the array as in our case (and therefore far below the cut-off frequency of the holes) and the thickness of the layer, the transmissivity is comparable to that of a continuous metal film. Here, the pitch of this array is roughly one tenth of the wavelength (λ) and the radius of the holes is smaller than $\lambda/40$ compared to the wavelength inside the dielectric layer at the studied frequency range therefore much below the traditional extraordinary transmission regime that appears when the wavelength is comparable to the periodicity or thickness of the holey film. In this case, the transmission through the free standing holey metal film would be expected to be negligible due to the mismatch between the fields of the impinging wave and the modes of the waveguides representing the holes even for small thicknesses. Furthermore, any excited mode inside these hole waveguides will present an exponential decay along the z axis due to them being far below cut off. Therefore, this system presents a lossless analogue of the impedance mismatch that limits the transmission through the sub-skin-depth homogeneous metal films, and hence we expect the cavity resonance to be able to overcome the limited transmission through the hole array.

In Fig. 8, we show the transmissivity curve for different hole radii obtained from the FEM modelling. It shows a monotonically increasing intensity of the transmission peak with the increasing radius of the holes, with a small shift to lower frequencies. It also shows that for a hole radius of 100 μm we obtain a transmissivity above 40% at 25 GHz when the cutoff of the fundamental mode of the holes is located above 900 GHz. Although this transmissivity maximum decays exponentially with the thickness, further modelling has shown that more than 20% of power transmission can be achieved for thicknesses up to 50 μm. It can also be seen that the transmission peaks for holey metal films present a shift toward lower frequencies, due to the inductive behaviour of the hole array, which affects the resonance frequency of the cavity. These results, together with the low angular dependence that was shown before, make this mechanism more suitable for practical applications that the traditional extraordinary transmission which is inherently angular dependent due to relying on the onset of diffraction.

In conclusion, we have studied the transmission through thin metal layers with and without an array of holes. We have presented an analytical procedure to solve this problem when the metal layer is simply modelled as a resistor due to its small thickness and high conductivity. We have obtained a very good agreement between FEM and experiment with our equivalent circuit model that validates our results, showing how a transmission peak of about 35% can be achieved, this peak moving little in frequency for any polarisation as the incident angle is changed up to 25°. With these characteristics, this device could be effectively used as a selective

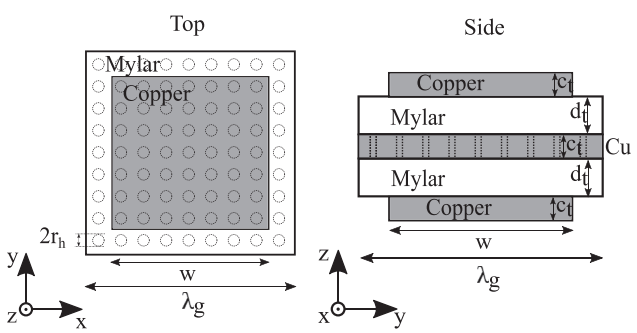

FIG. 7. Top and side views of the unit cell for the system comprising a holey metal film. The values of the parameters are $\lambda_g = 3.8$ mm, $w = 3.6$ mm, $d_t = 75$ μm and $c_t = 17$ μm.

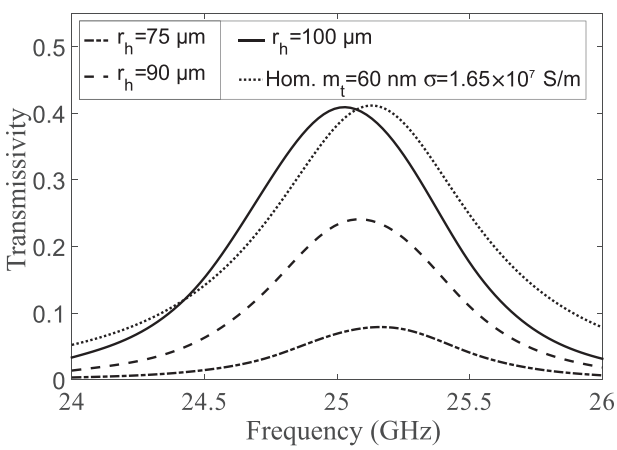

FIG. 8. FEM predictions of the transmissivity for normal incidence for the system illustrated in Fig. 7 for different hole radii in comparison to the case of normal incidence for the 60 nm homogeneous aluminium layer.

microwave filter. We have also extended the use of this impedance matching mechanism to achieve transmission through very subwavelength holes (with fundamental mode cut-off above 900 GHz) achieving a transmissivity peak of 40% at about 25 GHz, much below the well known extraordinary transmission peak that would be above 700 GHz.

The authors wish to acknowledge the financial support from the Engineering and Physical Sciences Research Council (EPSRC) of the United Kingdom, via the EPSRC Centre for Doctoral Training in Metamaterials (Grant No. EP/L015331/1). All data created during this research are openly available from the University of Exeter's institutional repository at https://ore.exeter.ac.uk/.

[1]I. R. Hooper, T. W. Preist, and J. R. Sambles, Phys. Rev. Lett. **97**, 053902 (2006).
[2]J. D. Edmunds, M. J. Lockyear, A. P. Hibbins, J. R. Sambles, and I. J. Youngs, Appl. Phys. Lett. **102**, 011120 (2013).
[3]A. P. Hibbins, J. R. Sambles, C. R. Lawrence, and J. R. Brown, Phys. Rev. Lett. **92**, 143904 (2004).
[4]B. A. Munk, *Frequency Selective Surfaces: Theory and Design* (Wiley, 2000).
[5]R. Florencio, R. R. Boix, and J. A. Encinar, IEEE Trans. Antennas Propag. **63**, 2558 (2015).
[6]M. Lambea and J. A. Encinar, "Analysis of multilayer frequency selective surfaces with rectangular geometries," in *9th International Conference on Antennas and Propagation (ICAP)*, Conf. Publ. No. 407 (Eindhoven, 1995), p. 528–531, Vol. 1.
[7]C. Molero, F. Medina, R. Rodríguez-Berral, and F. Mesa, Opt. Express **24**, 10265 (2016).
[8]R. Rodriguez-Berral, C. Molero, F. Medina, and F. Mesa, IEEE Trans. Microwave Theory Tech. **60**, 3908 (2012).
[9]COMSOL AB, "COMSOL Multiphysics®."
[10]J. Krupka, W. Strupinski, and N. Kwietniewski, J. Nanosci. Nanotechnol. **11**, 3358 (2011).
[11]T. W. Ebbesen, H. J. Lezec, H. F. Ghaemi, T. Thio, and P. A. Wolff, Nature **391**, 667 (1998).
[12]F. Medina, F. Mesa, and R. Marques, IEEE Trans. Microwave Theory Tech. **56**, 3108 (2008).
[13]F. J. García-Vidal, H. J. Lezec, T. W. Ebbesen, and L. Martín-Moreno, Phys. Rev. Lett. **90**, 213901 (2003).